

OPTIMIZATION OF A CIRCULAR MICROCHANNEL HEAT SINK USING  
ENTROPY GENERATION MINIMIZATION METHOD

ARASH JAFARI

A thesis submitted in fulfillment of the  
requirements for the award of the degree of  
Master of Engineering (Mechanical Engineering)

Faculty of Mechanical Engineering  
Universiti Technology Malaysia

MAY 2009

Dedicated to my beloved family and my mooshi.

## ACKNOWLEDGEMENT

My deepest gratitude is dedicated to Dr. Normah Mohd Ghazali, for her continued support, encouragement, and advice in supervising the research project. Her priciest guidance and unselfishly shared her opinion and knowledge are much appreciated.

## ABSTRACT

New advances in micro and nano scales are being realized and the contributions of micro and nano heat dissipation devices are of high importance in this novel technology development. Past studies showed that microchannel design depends on its thermal resistance and pressure drop. However, entropy generation minimization (EGM) as a new optimization theory stated that the rate of entropy generation should be also optimized. Application of EGM in microchannel heat sink design is reviewed and discussed. Using EGM, majority of the published investigations are conducted based on rectangular cross section microchannel. Latest principles for deriving the entropy generation correlations are discussed to present how this approach can be achieved. The present study involves an optimization procedure using EGM method and derives the entropy generation rate in circular microchannel heat sink based upon thermal resistance and pressure drop simultaneously. The equations are solved using MATLAB and the obtained results are compared to the past studies. The effect of channel diameter and number of channels on the entropy generation rate, Reynolds number, thermal resistance and pressure drop is investigated. Analytical correlations are utilized for heat transfer and friction coefficients. A minimum entropy generation has been observed for  $N=40$  and channel diameter of  $90\mu m$ . It is concluded that for  $N=40$  and channel hydraulic diameter of  $90\mu m$ , the circular microchannel heat sink is on its optimum operating point based on second law of thermodynamics.

## ABSTRAK

Penyelidikan pada skala mikro dan nano telah menjadi semakin maju dan sumbangan sistem mikro dan nano sebagai alat penenggelam haba saluran kini menjadi semakin penting. Kajian awal menunjukkan bahawa rekabentuk saluran mikro bergantung kepada rintangan haba dan susutan jumlah tekanan. Walaubagaimanapun, teori terbaru berkaitan penghasilan entropi minimum (EGM) menyatakan bahawa kadar penjanaan entropi juga perlu diambilkira. Aplikasi teori EGM dibincang di sini. Kajian ini merangkumi proses pengoptimuman menggunakan EGM dengan penerbitan kadar penjanaan entropi untuk sistem penenggelam haba saluran mikro berbentuk bulat berdasarkan rintangan haba dan susutan jumlah tekanan. Persamaan berkaitan diselesaikan dengan MATLAB dan perbandingan dilakukan dengan kajian terdahulu. Kesan-kesan garis pusat dan bilangan saluran terhadap penjanaan entropi, angka Reynolds, rintangan haba dan susutan jumlah tekanan telah dikaji. Teori sekaitan telah digunakan untuk pemindahan haba dan pekali geseran. Penjanaan entropi minima dikenal pasti berlaku pada jumlah saluran  $N = 40$  dan garis pusat  $90\mu m$ . Di sini boleh dirumuskan bahawa pada  $N = 40$  dan garis pusat  $90\mu m$ , penenggelam haba saluran mikro berbentuk bulat akan beroperasi pada tahap optima berdasarkan hukum kedua termodinamik.

## TABLE OF CONTENTS

CHAPTER	TITLE	PAGE
	DECLARATION	i
	DEDICATION	ii
	ACKNOWLEDGEMENT	iii
	ABSTRACT	iv
	ABSTRAK	v
	TABLE OF CONTENTS	vi
	LIST OF TABLES	viii
	LIST OF FIGURES	ix
	LIST OF SYMBOLS	xiv
	LIST OF APPENDICES	xix
<b>1</b>	<b>INTRODUCTION</b>	<b>1</b>
	1.1 Background	1
	1.2 Nanochannel	6
	1.3 Microchannel Heat Sink	11
	1.4 EGM Methodology	16
	1.5 Objective and Scopes	18

<b>2</b>	<b>THEROY</b>	<b>19</b>
	2.1 Theory	19
	2.2 Problem Definition	24
	2.3 Modelling and Governing Equations	27
<b>3</b>	<b>METHODOLOGY</b>	<b>35</b>
	3.1 Introduction	35
	3.2 Thermal Resistance Model	36
	3.3 Entropy Generation Model	48
	3.4 Total Pressure Drop	50
<b>4</b>	<b>RESULTS AND DISCUSSION</b>	<b>54</b>
	4.1 Effect of Channel Hydraulic Diameter on thermal resistance and pressure drop	54
	4.2 Effect of Channel Hydraulic Diameter on Entropy Generation Rate	72
<b>5</b>	<b>CONCLUSIONS AND RECOMMENDATIONS</b>	<b>81</b>
	5.1 Conclusions	81
	5.2 Recommendations	85
	<b>REFERENCES</b>	<b>86</b>
	<b>APPENDICES</b>	<b>91</b>

## LIST OF TABLES

TABLE NO	TITLE	PAGE
Table 1.1	Knudsen number ranges for various types of flow	3
Table 2.1	Microchannel heat sink dimensions	25
Table 2.2	The cooling water thermal properties	26
Table 4.1	Calculated data for $D_h$ of range $80\mu m$ to $103\mu m$ with $N=58$	56
Table 4.2	Equivalent channel hydraulic diameter of the circular channel regard to a rectangular channel of height $360\mu m$	62
Table 4.3	Equivalent channel hydraulic diameter of the circular channel regard to a rectangular channel of height $180\mu m$	63



## LIST OF FIGURES

FIGURE NO	TITLE	PAGE
Figure 1.1	The interdisciplinary field covered by the method of thermodynamic optimization, or entropy generation minimization.	4
Figure 1.2	A sketch of a nanochannel filled with a simple fluid. The filled circles denote the channel wall atoms, and the open circles denote the fluid atoms. The fluid atoms interact with each other by a Lennard–Jones potential $V_{LJ,1}$ , and the fluid atoms interact with the wall atoms by a Lennard–Jones potential $V_{LJ,2}$ .	7
Figure 1.3	Sketch of a typical radial distribution function (RDF) $g(r)$ . RDF measures the probability density of finding a particle at a distance $r$ from a given particle.	8

<b>FIGURE NO</b>	<b>TITLE</b>	<b>PAGE</b>
Figure 2.1	Circular microchannel heat sink and cross-section of its unit cell.	22
Figure 2.2	Structure of a circular microchannel heat sink and the unit cell	24
Figure 2.3	Entrance length of the microchannel for channel hydraulic diameter of range $80\mu m$ to $103\mu m$ with $N = 58$	27
Figure 2.4	entropy change of a control mass during an irreversible process	32
Figure 3.1	A circular microchannel control volume	37
Figure 3.2	A curved fin with adiabatic tip	39
Figure 3.3	circular channel and the simplified fin model	42
Figure 3.4	A model of microchannel convective heat transfer.	48
Figure 4.1	Effect of channel hydraulic diameter of range $80\mu m$ to $103\mu m$ with $N = 58$ on	55
Figure 4.2	Effect of channel hydraulic diameter of range $80\mu m$ to $103\mu m$ with $N = 58$ on total pressure drop	56
Figure 4.3	Effect of heat flux with channel diameter of range $80\mu m$ to $103\mu m$ and $N = 58$ on thermal resistance	58

<b>FIGURE NO</b>	<b>TITLE</b>	<b>PAGE</b>
Figure 4.4a	Effect of pumping power with channel diameter of range $80\mu m$ to $103\mu m$ and $N = 58$ on Reynolds Number	59
Figure 4.5	Effect of pumping power with channel diameter of range $80\mu m$ to $103\mu m$ and $N = 58$ on thermal resistance	61
Figure 4.6a	Effect of the equivalent channel hydraulic diameter of the circular channel regard to a rectangular channel of height $360\mu m$ on thermal resistance	64
Figure 4.7	Effect of the equivalent channel hydraulic diameter of the circular channel regard to a rectangular channel of height $180\mu m$ on thermal resistance	65
Figure 4.8a	Effect of the equivalent channel hydraulic diameter of the circular channel regard to a rectangular channel of height $360\mu m$ with $N=40$ on fin efficiency	66
Figure 4.9	Effect of the equivalent channel hydraulic diameter of the circular channel regard to a rectangular channel of height $360\mu m$ on pressure drop	67
Figure 4.10	Effect of the equivalent channel hydraulic diameter of the circular channel regard to a rectangular channel of height $180\mu m$ on pressure drop	68

<b>FIGURE NO</b>	<b>TITLE</b>	<b>PAGE</b>
Figure 4.11	Effect of $N$ on thermal resistance under channel hydraulic diameter constraint of range $40\mu m$ to $80\mu m$	69
Figure 4.12	Effect of $N$ on pressure drop under channel hydraulic diameter constraint of range $40\mu m$ to $80\mu m$	70
Figure 4.13	Effect of $N$ on fin efficiency under channel hydraulic diameter constraint $D_h = 40\mu m$	71
Figure 4.14a	Effect of channel hydraulic diameter of range $80\mu m$ to $103\mu m$ with $N = 58$ on entropy generation, $S_{gen}$	73
Figure 4.15	Effect of heat flux with channel diameter of range $80\mu m$ to $103\mu m$ and $N = 58$ on entropy generation, $S_{gen}$	74
Figure 4.16	Effect of pumping power with channel diameter of range $80\mu m$ to $103\mu m$ and $N = 58$ on entropy generation, $S_{gen}$	75
Figure 4.17a	Effect of the equivalent channel hydraulic diameter of the circular channel regard to a rectangular channel of height $360\mu m$ on entropy generation, $S_{gen}$	77
Figure 4.18a	Effect of the equivalent channel hydraulic diameter of the circular channel regard to a rectangular channel of height $180\mu m$ on entropy generation, $S_{gen}$	78
Figure 4.19	Effect of $N$ on entropy generation under channel hydraulic diameter constraint of range $40\mu m$ to $80\mu m$	79

## LIST OF SYMBOLS

$a$	-	fin height [m]
$b$	-	fin bottom width [m]
$A_c$	-	cross-section area of a circular channel [ $m^2$ ]
$A_{eff}$	-	total effective heat transfer area [ $m^2$ ]
$A_{(y)}$	-	cross-section area of a curved fin [ $m^2$ ]
$C_p$	-	specific heat of fluid [J/kg.K]
$D_h$	-	hydraulic diameter [m]
$E$	-	energy [J]
$\dot{E}$	-	energy rate [J/s]
$\Delta E$	-	energy change [J]
$f$	-	friction factor
$h$	-	specific enthalpy of the fluid [J/kg]
$h_{av}$	-	average heat transfer coefficient [ $W/m^2 \cdot ^\circ C$ ]
$k$	-	thermal conductivity of solid [ $W/m \cdot ^\circ C$ ]
$k_{eq}$	-	ratio of thermal conductivity of fluid to solid $\equiv k_f/k$
$k_f$	-	thermal conductivity of fluid [ $W/m \cdot ^\circ C$ ]
$Kn$	-	Knudsen number
$L_e$	-	entrance length [m]
$L_x$	-	total length of microchannel heat sink [m]

$L_y$	-	total height of microchannel heat sink [m]
$L_z$	-	total width of microchannel heat sink [m]
$m$	-	fin parameter [ $m^{-1}$ ]
$\dot{m}$	-	mass flow rate [kg/s]
$N$	-	total number of microchannels
$Nu_{D_h}$	-	Nusselt number based on hydraulic diameter
$P$	-	pressure [Pa]
$P_{(y)}$	-	fin perimeter [m]
$\bar{P}$	-	pumping power [W]
$\Delta P$	-	total pressure drop [Pa]
$Pe_{D_h}$	-	Peclet number based on hydraulic diameter
$Pr$	-	Prandtl number
$q$	-	wall heat flux [ $W/m^2$ ]
$q_w$	-	uniform wall heat flux [ $W/m^2$ ]
$Q$	-	heat transfer [J]
$\dot{Q}$	-	rate of heat transfer [W]
$\dot{Q}_b$	-	heat transfer rate from the base [W]
$\dot{Q}_{fin}$	-	heat transfer rate from the fin [W]
$r$	-	radial coordinate [m]
$r_0$	-	internal radius of microchannel [m]
$R$	-	gas constant [ $J/kg \cdot ^\circ C$ ]
$R_{th}$	-	thermal resistance [ $W/^\circ C$ ]
$Re_{D_h}$	-	Reynolds number based on hydraulic diameter

$S$	-	entropy [J/ °C]
$\dot{S}_{gen}$	-	total entropy generation rate [W/ °C]
$\dot{S}$	-	rate of entropy [J/ °C.s]
$\Delta S$	-	entropy change [J/ °C]
$s$	-	specific entropy of fluid [J/kg. °C]
$T$	-	temperature [ °C]
$T_o$	-	environment absolute temperature [K]
$t$	-	time [s]
$U_m$	-	mean velocity in channels [m/s]
$U$	-	internal energy [J]
$\Delta U$	-	change of internal energy [J]
$u$	-	specific internal energy [J/kg]
$\dot{V}$	-	total volume flow rate [ $m^3/s$ ]
$v$	-	specific volume of fluid [ $m^3/kg$ ]
$W$	-	work [J]
$W_{lost}$	-	work destruction [J]
$W_{pitch}$	-	width of pitch [m]
$\dot{W}$	-	rate of work [J/s]
$\dot{W}_{rev}$	-	rate of reversible work [J/s]
$x$	-	longitudinal coordinate [m]
$y$	-	longitudinal coordinate [m]

## Greek Symbols

$\Delta P$	-	pressure drop across microchannel
$\alpha$	-	thermal diffusivity [ $m^2/s$ ]
$\alpha_c$	-	channel diameter to microchannel heat sink width ratio
$\alpha_{hs}$	-	heat sink aspect ratio
$\beta$	-	channel diameter to channel pitch ratio
$\gamma$	-	ratio of specific heat $\equiv C_p/C_v$
$\mu$	-	absolute viscosity of fluid [ $kg/m.s$ ]
$\eta_{fin}$	-	fin efficiency
$\theta$	-	temperature difference, $T - T_\infty$ [ $^{\circ}C$ ]
$\theta_b$	-	base stream temperature, $T_b - T_a$ [ $^{\circ}C$ ]
$\nu$	-	kinematic viscosity of fluid [ $m^2/s$ ]
$\rho$	-	fluid density [ $kg/m^3$ ]
$\lambda$	-	mean free path of the gas

## subscripts

a	-	ambient
av	-	average
b	-	base
conv	-	convective
CV	-	control volume
eq	-	equivalent



f	-	fluid
fin	-	single fin
gen	-	generation
hs	-	heat sink
i	-	inner
in	-	entrance
int rev	-	internally reversible
lost	-	destruction
m	-	mean value
out	-	exit
rev	-	reversible
w	-	wall
1	-	initial
2	-	final

## LIST OF APPENDICES

APPENDIX	TITLE	PAGE
Appendix A-1	Measured Nusselt number from experimental results (Yang and Lin, 2007).	91
Appendix A-2	Friction factor from experimental results (Yang and Lin, 2007).	92
Appendix A-3	measured friction factor from experimental results for (a) fused silica tubes, and (b) stainless steel tubes (Li et al, 2007).	93
Appendix A-4	Local distribution of the Nusselt number of tube No.4 at different Reynolds (Li et al, 2007).	94
Appendix A-5	Local distribution of the Nusselt number of tube No.5 at different Reynolds (Li et al, 2007).	95
Appendix A-6	Local distribution of the Nusselt number of tube No.6 at different Reynolds (Li et al, 2007).	96
Appendix B-1	MATLAB R2008a Code	97
Appendix C-1	Effect of $\alpha_c$ with $\beta=0.6$ and $N=100$ ( $W_{pitch}=100 \mu\text{m}$ ) on (a) thermal resistance, and (b) total pressure drop (Abidin, 2006).	100

<b>APPENDIX</b>	<b>TITLE</b>	<b>PAGE</b>
Appendix C-2	Effect of (a) heat flux, and (b) pumping power at $\alpha_c$ of range 2 to 6 with $\beta=0.6$ and $N=100$ ( $W_{pitch}=100 \mu\text{m}$ ) on thermal resistance (Abidin, 2006).	101
Appendix C-3	Effect of $\beta$ on thermal resistance under channel height constraint, (a) $H_c=360\mu\text{m}$ , and (b) $H_c=180\mu\text{m}$ (Abidin, 2006).	102
Appendix C-4	Effect of $\beta$ on total pressure drop under channel height constraint, (a) $H_c=360\mu\text{m}$ , and (b) $H_c=180\mu\text{m}$ (Abidin, 2006).	103
Appendix C-5	Effect of $N$ on (a) thermal resistance, and (b) total pressure drop under channel height constraint, $H_c=360\mu\text{m}$ (Abidin, 2006).	104
Appendix C-6	Effect of $\alpha_c$ of range 2 to 6 with $\beta=0.6$ and $N=100$ ( $W_{pitch}=100 \mu\text{m}$ ) on entropy generation, $S_{gen}$ (Abidin, 2006).	105
Appendix C-7	Effect of (a) heat flux, and (b) pumping power for $\alpha_c$ of range 2 to 6 with $\beta=0.6$ and $N=100$ ( $W_{pitch}=100 \mu\text{m}$ ) on entropy generation, $S_{gen}$ (Abidin, 2006).	106
Appendix C-8	Effect of $\beta$ on entropy generation under channel height constraint, (a) $H_c=360\mu\text{m}$ , and (b) $H_c=180\mu\text{m}$ (Abidin, 2006).	107

<b>APPENDIX</b>	<b>TITLE</b>	<b>PAGE</b>
Appendix C-9	Effect of $N$ on entropy generation under channel height constraint, (a) $H_c=360\mu\text{m}$ , and (b) $H_c=180\mu\text{m}$ (Abidin, 2006).	108

## CHAPTER 1

### INTRODUCTION

#### 1.1 Background

Micron- and submicron-size mechanical and biochemical devices are becoming more prevalent both in commercial applications and in scientific inquiry. Small accelerometers with dimensions measured in microns are being used to deploy air bag systems in automobiles. Tiny pressure sensors for the tip of a catheter are smaller than the head of a pin. Microactuators are moving scanning electron microscope tips to image single atoms. Novel bioassays consisting of microfluidic networks are designed for patterned drug delivery. New fabrication techniques, such as surface silicon micromachining, bulk silicon micromachining, Lithographie Galvanoformung Abformung (LIGA), and Electro Discharge Machining (EDM) have been successfully applied to micro fabrication in recent years, making these microdevices possible. The capability to batch fabricates and automate these fabrication technologies makes such microdevices inexpensive. New nanofabrication techniques have emerged exploiting the concept of self-assembly for submicron-size objects.

The operation of most of the electronic devices is strongly influenced by their temperature and the thermal environment near them. As an example, the present computer technology owes much of its progress to the miniaturization of circuits of

silicon chip. The demand for faster circuits and increased capacity, has led to an increase in power densities and a need for continuous improvement in the methods of heat removal.

Microchannel heat sink is known for its excellent cooling capacity due to the high surface to volume ratio that enhances heat removal. Tuckerman and Pease first realized the potential of this technology and initialled the foundation for silicon based micro-channel heat sink experimentation (Tuckerman, D.B., and Pease, R.F.W., 1981). Later on Samalam reported correlations for thermal resistance (Samalam, V.K. 1989) based on the theoretical study of the experiments by Tuckerman. Fedorov and Viskanta carried out numerical simulation (Fedorov, A.G., Viskanta, R., 1999) based on the experimental data. Qu and Mudawar computed a 3-D fluid flow and heat transfer study on micro-channel with rectangular cross-section (Mudawar, I., and Qu, W., 2002). Li et al. numerically investigated 3-D conjugate heat transfer in a silicon based micro-heat sink [2-D fluid flow and 3-D heat transfer] (Li et al, 2004). Toh et al. (Toh et al., 2002) carried out the detailed numerical study of variation of local thermal resistance and friction factor along the flow direction in micro-channels of different cross-section (Toh et al., 2002). Li and Peterson parametrically optimized the micro-channel geometry for various numbers of channels and cross-sections of micro channel (Li and Peterson, 2006). The major part of works was to investigate the microchannels design parameters. Micro channels are normally known for their low Reynolds numbers, high pressure drop and heat transfer coefficient. Kandlikar S.G. (Kandlikar S.G., 2003) in their paper discussed the importance of rarefaction effects in gas flow, electric double layer, entrance region, developing flows and experimental errors in microchannels study. One of the important parameters in microchannel study is the Knudsen number (**Kn**) which is a measure of the departure from the continuum. Knudsen number is defined as the ratio of the mean free path of the gas to the hydraulic diameter of the flow channel

$$(\mathbf{Kn} = \frac{\lambda}{D_h}) \quad (1.1)$$

Based on the Knudsen number, various types of flows may be defined. The results are summarized in Table 1.1 .

Table 1.1 Knudsen number ranges for various types of flow (Kandlikar S.G., 2003)

<b>Rang of Knudsen Numbers</b>	<b>Type of Flow</b>
<b>0.001&gt;Kn</b>	<b>Continuum Flow:</b> no rarefaction effects
<b>0.1&gt;Kn&gt;0.001</b>	<b>Slip Flow:</b> rarefaction effects that can be modelled with a modified continuum theory accounting for wall slip
<b>10&gt;Kn&gt;0.1</b>	<b>Transition Flow:</b> a type of flow between slip flow and free molecular flow that is analyzed statistically; i.e. with Boltzman equation
<b>Kn&gt;10</b>	<b>Free Molecular Flow:</b> motion of individual molecules must be modelled and then treated statistically

Thermodynamic optimization or entropy generation minimization (EGM) of systems involves analysis of multidisciplinary areas of heat transfer, engineering thermodynamics, and fluid mechanics. The position of the field may be described by Figure 1.1. Principles of heat and mass transfer, fluid mechanics, and engineering thermodynamics are simultaneously applied to model processes, devices, and installations which account for the inherent irreversibility of engineering systems and processes. Entropy generation is similar to exergy destruction; but with difference of relying on heat transfer and fluid mechanics, as well as thermodynamics.

For a general system-environment configuration based on Gouy-Stodola theorem (Bejan A., 1996a),

$$\dot{W}_{\text{rev}} - \dot{W} = T_o \dot{S}_{\text{gen}} \quad (1.2)$$

The lost power ( $\dot{W}_{\text{rev}} - \dot{W}$ ) is always positive, regardless of whether the system is a power producer (e.g. power plant) or a power user (e.g. refrigeration plant). Minimizing the lost power is the same as maximizing the power output in a power plant, and minimizing the power input in a refrigeration plant. This operation is also equivalent to minimizing the total rate of entropy generation.

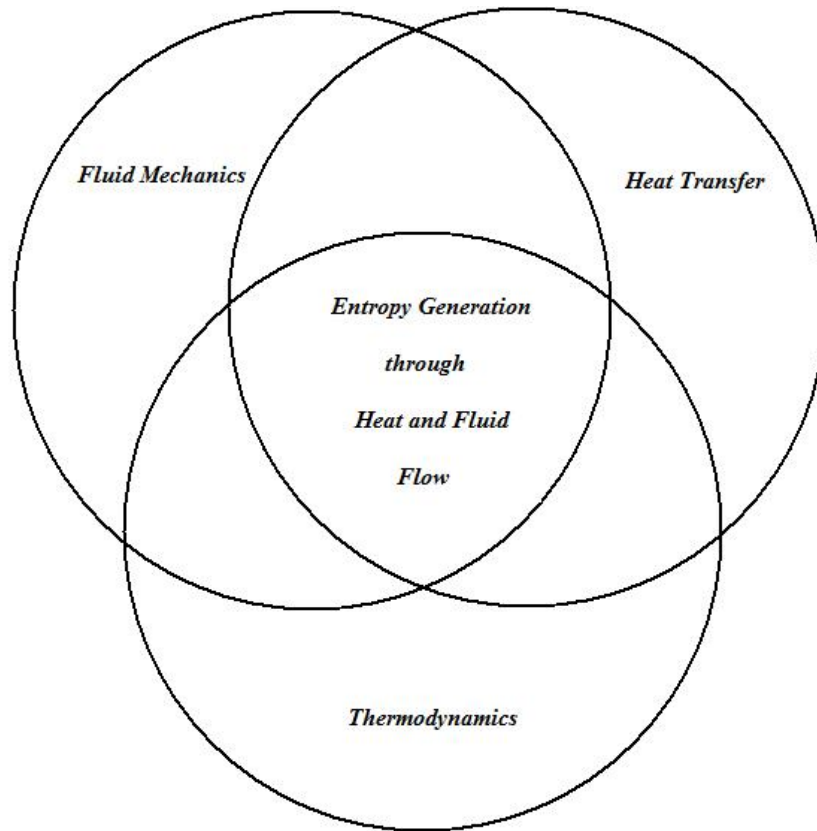


**(FIGURE 1.1)** The interdisciplinary field covered by the method of thermodynamic optimization, or entropy generation minimization.

The critically new aspect of the EGM method is from the pure exergy analysis in the optimization and design (the generation of structure). To minimize the irreversibility of a proposed configuration, the analyst must use the relations between temperature differences and heat transfer rates, and between pressure differences and mass flow rates. The design  $\dot{S}_{gen}$  is then expressed as a function of the topology and physical characteristics of the system, namely, finite dimensions, shapes, materials, finite speeds, and finite-time intervals of operation. For this the optimization has to be conducted on heat transfer and fluid mechanics principles, in addition to thermodynamics.

Nano-fluidic systems and hybrid micro/ nano fluidic systems have attracted considerable attention in recent years. A review of the literature, however, shows that structure and geometry of nanochannel has been paid relatively less attention for investigation. In nanoscale systems, the surface-to-volume ratio is very high, and the critical dimension can be comparable to the size of the fluid molecules. The influence of the surface and the finite-size effect of the various molecules on fluid transport



needs to be understood in detail, while such effects may be largely neglected for liquid flows in macroscopic channels.

## 1.2 Nanochannel

With the growing interest in the development of faster, smaller and more efficient biochemical analysis devices, nanofluidics systems and hybrid micro/nano fluidics systems have attracted considerable attention in recent years. A key difference between the simulation of the fluidics transport in confined nanochannels, where the critical channel dimension can be a few molecular diameters, and at macroscopic scales is that the well-established continuum theories (Navier-Stokes equations) may not be valid in confined nanochannels. Therefore, atomistic scale simulations, in which the fluid atoms are modelled explicitly, and the motion of the fluid atoms is calculated directly, give fundamental insights on fluid transport. The most popular technique for atomistic simulation of liquid transport is molecular dynamics (MD).

Two major kinds of flow in nanochannels are “simple fluid flow and water flow” which are of high importance in nanochannel study. Simple fluid is a collection of molecules that interact via the Leonard-Jones potential which will be defined later. The dynamics follow the classical mechanics (Newton’s second law). In practice some noble gases (e.g., argon) can be modelled fairly accurately as a simple fluid. Main advantages of the study of simple fluids are:

1. Much lower computational cost is required compared to complex fluids.
2. Despite its simplicity, it has a deeper insight into physics of fluid transport in nanochannels.
3. Generates data for validation of theories describing fluid transport in nanochannels

Simple fluids can be described by the Lennard-Jones (LJ) potential:

$$V_{LJ} = 4\varepsilon \left[ \left( \frac{\sigma}{r} \right)^{12} - \left( \frac{\sigma}{r} \right)^6 \right] \quad (1.3)$$

Where  $\varepsilon$  is related to the interaction strength,  $\sigma$  is the interaction length scale and  $r$  is the distance. Since forces due to LJ potential can be evaluated numerically and describes the interaction between nonpolar molecules quite well, LJ is the most popular interaction potential used in MD simulations. In the MD simulation of LJ fluids, the physical quantities are computed using reduced units.

Depending on the critical length scale of the channel, the fluidic transport behaviour can either deviate significantly from the classical continuum theory prediction or be very similar to the transport of a bulk fluid described by the classical theory. These observations follow from the fact that when the fluid atoms are confined to molecular channels, the fluid can no longer be taken to be homogeneous, and strong oscillations in fluid density occur near the fluid-solid interface. Therefore, the dynamic behaviour of the fluid significantly differs from that of the bulk.

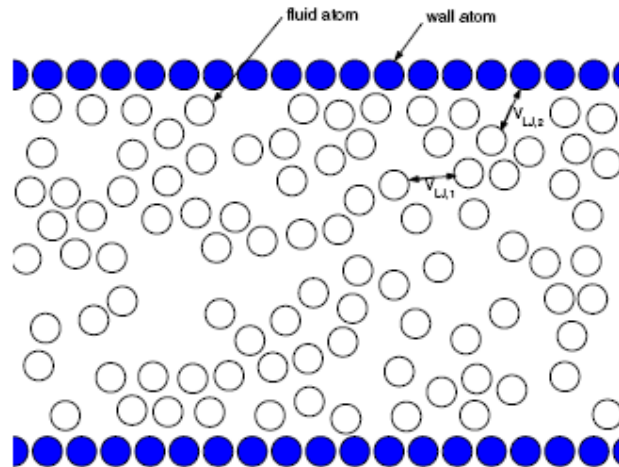


**(FIGURE 1.2)** A sketch of a nanochannel filled with a simple fluid. The filled circles denote the channel wall atoms, and the open circles denote the fluid atoms. The fluid atoms interact with each other by a Lennard–Jones potential  $V_{LJ,1}$ , and the fluid atoms interact with the wall atoms by a Lennard–Jones potential  $V_{LJ,2}$ . Karniadakis (Karniadakis et al., 2005)

Some features which must be considered for a simple fluid MD simulation;

**Density Distribution-** The strong density oscillation of fluid atoms near the fluid/solid interface are a universal phenomenon which has been observed in almost all MD simulations of nanofluidic flows and has been verified experimentally

**Radial Distribution Function-** Density fluctuation near a channel wall can be expressed using the concept of a radial distribution function (RDF). RDF ( $g(r)$ ) measures the probability density of finding a particle at a distance of  $r$ . The fluid layering near the channel wall is mainly induced by the structure of fluid RDF and the structure of the solid wall.

Simple fluids in nanochannels are inhomogeneous because of the strong layering of fluid atoms near the channel wall. Classical fluid transport theories do not account for the inhomogeneity of the fluid, and transport parameters such as

diffusivity and viscosity are strongly influenced by the fluid layering in nanochannels. Fluid layering can be influenced by various parameters such as the wall structure, fluid-wall interactions, and channel width.

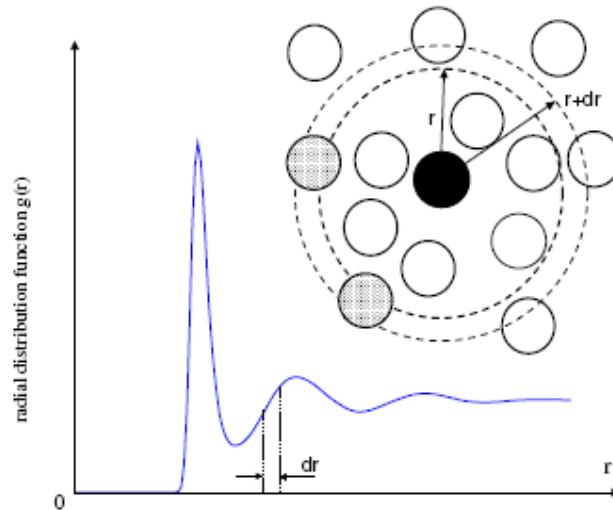


**(FIGURE 1.3)** Sketch of a typical radial distribution function (RDF)  $g(r)$ . RDF measures the probability density of finding a particle at a distance  $r$  from a given particle ( $r = 0$  corresponds to the position of the given particle). Karniadakis (Karniadakis et al., 2005)

**Fluid-Wall Interactions-** The interaction between a fluid atom and a wall atom is usually modelled by LJ potential. The LJ parameters for fluid-fluid and fluid-wall interactions are denoted by  $(\epsilon, \sigma)$  and  $(\epsilon_{wf}, \sigma_{wf})$  respectively. A higher  $\epsilon_{wf}$  corresponds to stronger interaction between the fluid and wall atoms.

**Effects of Nanochannel width-** it is found that for channels wider than  $10\sigma$ , the fluid layers near the wall are independent of channel width and the central fluid behaves more like bulk fluid.

**Structure of the Wall Atoms-** Smooth walls as well as walls with atomistic structure have been widely used in the MD simulation of nanofluid confined in nanoscale channels. It has been realized that for smooth wall, the wall-fluid potential depends on the normal distance between the fluid atom and the channel wall, whilst for a wall with atomistic structure, the wall-fluid potential depends on the relative distance between the fluid atom and each atom wall.

**Diffusion Transport-** Diffusion transport is typically important in most nanofluidic systems. This can be understood by Peclet number, indicating that diffusion can either dominates the transport or is as important as the bulk transport.

**Validity of the Navier-Stokes Equations-** During the last several years, researchers have used MD simulations to test the accuracy of the Navier-Stokes equations in nanochannels (Koplik et al., 1987, Travis and Gubbins, 2000). In the continuum fluid transport theory governed by Navier-Stokes equations, it is assumed that the state variables (density, temperature) do not vary appreciably over length and timescale comparable to the molecular free path and molecular relaxation time. It was shown that the fluid density near the solid-liquid interface can vary significantly over intermolecular distances. While these local density oscillations may not necessarily mean the breakdown of the continuum theory, it is important to understand how the continuum theory works for liquids in confined channels.

**Boundary Conditions at Solid-Liquid Interfaces-** It is shown that the MD simulations systemically underpredict the slip length deduced from various experiments, specifically, predict a slip length roughly ten times smaller than in the experiments. Such a large discrepancy implies that there are some other physical phenomena not included in the simulation. Molecular slippage, gaseous film, no-shear/no-slip patterning and viscosity model are other conceptual models of slip.

**Molecular Dynamics (MD) Method-** This is suitable for simulating very small volumes of liquid flows, with linear dimensions on the order of 100nm or less and for time intervals of several tenths of nanoseconds. It can deal effectively with nanodomains and it is perhaps the only accurate approach in simulating flows involving very high shear where the continuum may not be valid. For dimensions less than approximately ten molecules, the continuum hypothesis breaks down even for liquids and MD should be employed to simulate the atomistic behaviour of such a system. MD is, however, inefficient for simulating microflows due to the large intermolecular distances that require relatively large distances. Gas microflows are simulated more efficiently using direct simulation Monte Carlo (DSMC) method. Another emerging application of MD simulation is investigation of the fluid thermal behaviour of nanotubes.

Molecular dynamics (MD) computes the trajectories of particles that model the atoms of the system, since they result from relatively simple force fields. The MD simulations generate a sequence of points in phase space as a function of time, these points belong to the same ensemble, and they correspond to the different conformations of the system and their respective momenta. An ensemble is a

collection of points in phase space satisfying the conditions of particular thermodynamics state. Several ensembles, with different constraints on the thermodynamic state of the system are commonly used in MD.

The motion of an ensemble of atoms in MD simulations is governed by interatomic forces arising from interaction of electrons and nuclei. Thus, the results obtained from MD simulations are linked with ability of the potential energy function to represent the underlying system. In classical MD simulation, first, a model system consisting of  $N$  particles is selected and Newton's equations of motion are solved until the properties of the system no longer change with time. Once a steady state is reached, the required measurements are performed.

The key steps in MD simulation are:

1. **Initialization:** Initial positions and velocities must be assigned to  $N$  particles.
2. **Force calculation:** Forces due to the interactions are computed.
3. **Integration of the equations of motion:** Verlet integration rule
4. **Data storage and analysis:** After the equations of motion are integrated, the relevant properties of the system (temp., press...) are calculated and then stored.

The definition of accurate intermolecular potentials is the key to any atomistic simulation, and therefore, for MD simulation. Consequently, calculation of the potential function and the associated force accounts for most of the computational cost in an atomistic simulation. As a result, it is considered as one of the major components during the nano investigations.

Published studies currently available show that nanoscale devices and nanochannels design technology is in the earliest stages. Governing theories have not been really established and for some, microscale and nanoscale systems considered as one and the same. Thus this study will look into the entropy minimization of a microchannel system, specifically the circular geometry design. Since the fluidic transport behaviour involve similar characteristics, the results obtained may be conservatively used in the nanochannel study.

### 1.3 Microchannel Heat Sink

The problem of achieving compact, high-performance forced liquid cooling of integrated circuits first was investigated by Tuckerman and Pease (Tuckerman and Pease, 1981). They found that for laminar flow in confined channels, the use of high-aspect ratio channels for increased surface area will, to an extent, further reduce thermal resistance. Based on this consideration, a compact, water-cooled integral heat sink for silicon integrated circuits was designed and tested. The experimental work revealed the capability of heat dissipation up to a maximum power of  $790 \text{ W/cm}^2$  of the compact water-cooled heat sink. Since that experiment, there have been many experimental and analytical investigations on microchannel heat sinks and their thermal and fluidic performances.

Later on Knight (Knight et al, 1991) showed that for a fully developed flow in closed finned channels, there was an optimal geometrical design of the size and number of cooling channels to increase the heat transfer. Using maximum allowable pressure drop through the cooling channels, an optimization scheme was described and was compared with previously published case by Tuckerman and Pease (1981) for water-cooled Silicon wafers. Results showed that a significant reduction of thermal resistance was obtained by using fin/channel dimensions. Beside that work, Knight (Knight et al, 1992) tried to develop theoretical optimization procedures to minimize the overall thermal resistance of microchannel heat sinks for a given pressure drop. He presented the governing equations for fluid dynamics and heat transfer in the heat sink in a dimensionless form and then presented a scheme for solving these equations. Solution procedure for both laminar flow and turbulent flow through the channels was presented.

A high performance forced air cooling scheme was investigated theoretically and experimentally by Kleiner (Kleiner et al, 1995) which was employing microchannel parallel plate-fin heat sinks using air. During the work sample heat sinks with lateral dimensions of  $5 \times 5 \text{ cm}^2$  and fin lengths of 1.5 and 2.5 cm were fabricated from copper and aluminium foils and cooling system performance was modelled in terms of thermal resistance, pressure drop, and pumping power. A fin thicknesses and channel widths on the order of 200 and 500  $\mu\text{m}$ , respectively was used and Thermal resistances at the rate of 0.2 R/W was measured. In comparison

with the prior works dealing with direct air cooling, it was concluded that the investigated cooling approach possessed an acceptable performance.

Some three-dimensional models have also been developed. Continuum model derived from Navier-Stokes equation has been applied numerically to illustrate the transport mechanism of micro channel heat sinks. The work done by Federov and Viskanta (Federov and Viskanta, 1999) was to investigate flow and conjugate heat transfer in the microchannel-based heat sink for electronic packaging applications. The incompressible laminar Navier–Stokes equations of motion were employed as the governing conservation equations which were solved numerically using finite-volume method. The validation of the theoretical model developed was done by comparing thermal resistance and the friction coefficient with available experimental data for a wide range of Reynolds numbers. The analysis shed a unique fundamental insight into the complex heat flow pattern established in the channel due to combined convection–conduction effects in the three-dimensional setting.

The other investigation on three-dimensional numerical analysis was carried out to analyse fluid flow and heat transfer in a rectangular micro-channel heat sink numerically using water as the cooling fluid. Qu and Mudawar (Qu and Mudawar, 2002) simulated a heat sink which consist of a 1-cm<sup>2</sup> silicon wafer with micro-channels width of 57  $\mu\text{m}$  and depth of 180  $\mu\text{m}$ . They also developed a numerical code based on the finite difference method and the SIMPLE algorithm to solve the governing equations and validated by comparing the predictions with analytical solutions and available experimental data. It was found that the temperature rise along the flow direction in the solid and fluid regions can be approximated as linear. Flow Reynolds number affects the length of the flow developing region .It was concluded that for a relatively high Reynolds number of 1400, fully developed flow may not be achieved inside the heat sink. Although the classical fin analysis method is a simplified means to modelling heat transfer in micro-channel heat sinks, some key assumptions introduced in the fin method deviated significantly from the real situation, which could compromise the accuracy of the method. It was also understood that increasing the thermal conductivity of the solid substrate reduces the temperature at the heated base surface of the heat sink, especially near the channel outlet.



In another study, Qu and Mudawar (Qu and Mudawar, 2002) tested a microchannel heat sink 1cm wide and 4.8cm long. The microchannels machined in the heat sink were 231 $\mu\text{m}$  wide and 712 $\mu\text{m}$  deep. Apart from this they also presented numerical analysis for a unit cell containing a single microchannel and surrounding solid. The measured pressure drop across the channels and temperature distribution showed good agreement with the numerical results. They concluded that the conventional Navier-Stokes and energy equations remain valid for predicting fluid flow and heat transfer characteristics in microchannels.

Ryu (Ryu et al, 2002) performed numerical optimization of thermal performance of microchannel heat sinks. The objective of the optimization was to minimize thermal resistance. They varied the channel width, channel depth and the fin thickness to come up with an optimized solution. Their observation was that the channel width is the most important parameter dictating the performance of a microchannel heat sink.

Different works have been conducted to investigate the effect of micro channel heat sink geometry on its performance. Upadhye and Kandlikar (Upadhye and Kandlikar, 2004) analyzed direct cooling of an electronic chip of a function of channel geometry for single-phase flow of water. With fully developed laminar flow consideration and constant wall temperature and constant channel wall heat flux boundary conditions, the effect of channel dimensions on the pressure drop, the outlet temperature of the cooling fluid and the heat transfer rate was presented. A few conclusions were made. The results indicated that a narrow and deep channel results in improved heat transfer performance for a given pressure drop constraint.

One of the most comprehensive three dimensional model was developed by Li et al. (Li et al, 2004) A detailed numerical simulation of forced convection heat transfer occurring in silicon-based microchannel heat sinks was conducted using a simplified three-dimensional conjugate heat transfer model with a 2D fluid flow and 3D heat transfer. This model was developed using a finite difference numerical code with a Tri-Diagonal Matrix Algorithm (TDMA) to solve the governing equations and provided detailed temperature and heat flux distributions in the microchannel heat sink. The investigation was done to understand the influence of the geometric parameters of the channel and the thermo physical properties of the fluid on the flow

and heat transfer. The results were presented and it was found that thermo physical properties of the liquid can significantly influence both the flow and heat transfer in the microchannel heat sink. Apart from that work, Li and Peterson (Li and Peterson, 2006) investigated the most optimized geometry of a microchannel with liquid flow for the same numerical model as Li et al. (Li et al, 2004). It was concluded that the optimal number of channels was 120 per cm with the largest possible aspect ratio.

Another investigation on a three dimensional model was conducted by Lee and Garimella (Lee, P.S, and Garimella, 2006) which was a three-dimensional numerical simulations for laminar thermally developing flow in microchannels of different aspect ratios. It was completed under laminar convective heat transfer in the entrance region of microchannels of rectangular cross-section consideration with circumferentially uniform wall temperature and axially uniform wall heat flux thermal boundary conditions. The local and average Nusselt numbers were presented as a function of the dimensionless axial distance and channel aspect ratio depending on the temperature and flux distributions obtained. The advantage of the investigation was that generalized correlations, useful for the design and optimization of microchannel heat sinks and other microfluidic devices, was proposed for predicting Nusselt numbers

Beside the various experimental, analytical and numerical works done on the thermal performance and pressure drops of the microchannel heat sinks, other experimental, analytical and numerical studies were pioneered to investigate the effect of microchannel geometry, apart from rectangular cross section, on the microchannel heat sink. The most popular experiments were those done with trapezoidal cross section. Qu et al. (Qu et al, 1999) conducted two simultaneous experiments to investigate flow and heat transfer characteristics of water through trapezoidal silicon microchannels with a hydraulic diameter ranging from 51 to 169  $\mu\text{m}$ . A numerical analysis was also carried out by solving a conjugate heat transfer problem involving simultaneous determination of the temperature field in both the solid and the fluid regions. The experimental results were compared with the numerical predictions of heat transfer field and with the predictions from the conventional laminar flow theory. A significant difference between the experimental data and the theoretical predictions was found. Experimental results indicated that pressure gradient and flow friction in

microchannels are higher than those given by the conventional laminar flow theory and the experimentally determined Nusselt number is much lower than that given by the numerical analysis. The measured higher pressure gradient, flow friction and lower Nusselt numbers are due to the effect of surface roughness of the microchannels (Qu et al, 1999).

A numerical study devoted to the hydraulic properties of a network of parallel triangular microchannels was presented by Niklas et al. (Niklas et al, 2005) with hydraulic diameter of 110  $\mu\text{m}$ . Previous experimental investigations had revealed that pressure drop through the microchannels system dramatically increases for the Reynolds number exceeding 10. Numerical simulations were performed by using the classical system of continuity and Navier-Stokes equations and showed a very good agreement with the experimental results proving that there is no scale effect for the microchannels considered. It was also clearly indicated that the excessive pressure losses in the high Reynolds number range are due to the secondary flows and separations appearing in several regions of the microchannel system.

A thermal investigation of a polymeric microchannel heat sink was conducted by Barba et al. (Barba et al, 2005). A geometrical configuration consisting of a circular microduct with a gas running through it was designed and a three-dimensional procedure was developed to solve the model. The conjugate heat transfer problem was solved assuming fully developed laminar flow in forced convection and considering a gas flow with low Prandtl and Reynolds numbers with a numerical solution obtained for 2-D coordinates. The theoretical results were compared with experimental data concerning helium and nitrogen flows in circular microducts and good agreements were concluded.

## 1.4 EGM Methodology

Bejan first introduced optimization of heat sink using EGM in 1996(Bejan, 1996b). It was found that entropy generation associated thermal resistance and fluid friction effects, directly evaluate the amount of lost potential for work which in a heat sink system is equal to the lost ability of system to transfer heat to the surrounding. He also introduced the fundamentals of the methods of exergy analysis and entropy generation minimization (Bejan, 2001). The proportionality between exergy destruction and entropy generation was illustrated by examples of open and closed systems. Since then there have been some other investigations to utilize EGM principles to heat sink applications. One of the major works was done by Sahin (Sahin, 1998) where he applied the method to macro scale ducts with different geometries considering constant heat flux and laminar flow. It was concluded that if the frictional contribution of entropy generation become significant, the circular duct showed the best performance. Ogiso (Ogiso, 2001) presented a method of assessing the overall cooling performance in the thermal design of electronics. The method was based on the optimization concept of EGM. In comparison with experimental and numerical data it was found that the overall cooling performance is increased with decreasing entropy generation rate.

Culham and Muzychka (Culham and Muzychka, 2001) presented a procedure that allowed the simultaneous optimization of heat sink design parameters based on a minimization of the entropy generation associated with heat transfer and viscous dissipation. All relevant design parameters for plate fin heat sinks, including geometric parameters, heat dissipation, material properties and flow were simultaneously optimized to characterize a heat sink that minimizes entropy generation and in turn results in a minimum operating temperature. For the imposed problem constraints the model was shown to converge to a unique solution that gave the optimized design conditions.

Ratts and Raut (Ratts and Raut, 2004) obtained an optimal Reynolds number for laminar and turbulent flow in tubes considering EGM method to optimize a single-phase, convective, fully developed flow with uniform and constant heat flux. The

study also compared the optimal Reynolds number and minimum entropy generation for cross sections: square, equilateral triangle, and rectangle with aspect ratios of two and eight. The authors made a very interesting conclusion that rectangle with aspect ratio of eight had the smallest optimal Reynolds number, the smallest entropy generation number, and the smallest flow length. The present study will utilize these principles to apply the EGM method to different microchannel geometry apart from rectangle.

A numerical investigation was carried out on the entropy generation due to the steady laminar forced convection fluid flow through parallel plates microchannel by Haddad et al. (Haddad et al. 2004) The study was to discuss the effect of Knudsen, Reynolds, Prandtl, Eckert numbers and the non-dimensional temperature difference on entropy generation within the microchannel. It was based on the Bejan number. It was found that the entropy generation within the microchannel decreases as Knudsen number increases, and increases as Reynolds, Prandtl, Eckert numbers and the non-dimensional temperature difference increase. They concluded that the contribution of the viscous dissipation in the total entropy generation increases as Knudsen number increases over wide ranges of the flow controlling parameters.

Most of optimization objectives of microchannel heat sink were to minimize thermal resistance for a given pressure drop or to minimize the pump power for a specified thermal resistance. Khan et al. (Khan et al., 2006) employed the EGM procedure to optimize the overall performance of microchannel heat sinks which allowed the combined effects of thermal resistance and pressure drop to be assessed simultaneously as the heat sink interacts with the surrounding flow field. Air was used as the cooling fluid in the analysis. The variation of entropy generation rate in the slip flow region was investigated by altering the aspect ratio, fin spacing ratio, heat sink material, Knudsen numbers and accommodation coefficients of microchannels. It was illustrated that volume mass flow rate and channel aspect ratio strongly affected the entropy generation of three different Knudsen number. Based on new general expressions developed by Khan et al. (Khan et al, 2006) for the entropy generation rate, an analytical investigation made use the same principle of minimization of entropy generation (Abidin U, 2006).

## 1.5 Objective and Scopes

The present study will investigate the application of the entropy generation minimization method to a circular microchannel heat sink.

The principle of entropy generation relations in circular microchannels will be inspected. A dimensionless average entropy generation in the circular cross section will be derived. The ultimate objective is to optimize the circular microchannel heat sink based on entropy generation minimization. The scopes of this study can be summarized as

1. To review works on optimization of circular microchannel heat sink.
2. To derive the dimensionless average entropy generation rate in a circular microchannel.
3. To derive the principle entropy generation minimization correlation for a circular microchannel heat sink.
4. To compare the derived correlation and obtained results with other numerical and experimental works.